ELSEVIER

Physica D 148 (2001) 317–335

PHYSICA D

www.elsevier.com/locate/physd

Seasonally forced disease dynamics explored as switching between attractors

Matt J. Keeling*, Pejman Rohani, Bryan T. Grenfell

Zoology Department, University of Cambridge, Downing Street, Cambridge CB2 3EJ, UK

Received 25 July 2000; received in revised form 2 October 2000; accepted 2 October 2000
Communicated by Y. Kuramoto

Abstract

Biological phenomena offer a rich diversity of problems that can be understood using mathematical techniques. Three key features common to many biological systems are temporal forcing, stochasticity and nonlinearity. Here, using simple disease models compared to data, we examine how these three factors interact to produce a range of complicated dynamics. The study of disease dynamics has been amongst the most theoretically developed areas of mathematical biology; simple models have been highly successful in explaining the dynamics of a wide variety of diseases. Models of childhood diseases incorporate seasonal variation in contact rates due to the increased mixing during school terms compared to school holidays. This 'binary' nature of the seasonal forcing results in dynamics that can be explained as switching between two nonlinear spiral sinks. Finally, we consider the stability of the attractors to understand the interaction between the deterministic dynamics and demographic and environmental stochasticity. Throughout attention is focused on the behaviour of measles, whooping cough and rubella.

Keywords: Childhood diseases; Stochasticity; Seasonal forcing; SIR models; Nonlinearity

1. Introduction

Epidemiology has been one of the most successful quantitative branches of ecology. In particular, the study of childhood infections using the SIR (susceptible–infectious–recovered) family of models has yielded many mathematically interesting results [1–4] and shown good agreement with observations of disease case reports [5–12]. The rich variety of dynamics observed arise through three-way interactions between nonlinearities (due to the mixing of susceptible and infectious individuals), stochasticity (both demographic and environmental) and temporal forcing (caused by changes in the average contact rate).

The deterministic SIR model [5,7,13] and more complex variations on this theme [6,11,14] all demonstrate qualitatively similar dynamical properties. In general, this family of models possess a globally stable fixed point attractor in a homogeneous environment, and shows large amplitude oscillations when seasonally forced, often producing period-doubling cascades as the level of seasonality is increased [15–17]. Numerous authors have observed the signature of seasonal forcing in the number of reported cases [18,19] while others have found the magnitude and form of seasonal forcing to be important for obtaining both quantitative and qualitative agreement with observations [6,9,13,20].

* Corresponding author. Tel.: +44-1223-336644; fax: +44-1223-334466.
E-mail address: matt@zoo.cam.ac.uk (M.J. Keeling).

0167-2789/01/$ – see front matter
PII: S0167-2789(00)00187-1

Periodically forced nonlinear oscillators have been studied extensively in the mathematical literature [21–26], with many examples motivated by biological processes [27–32]. However, much of the theory relates to limiting cases where either the forcing is small, or the period is close to the resonant frequency of the oscillator. For realistic disease models we are not afforded such convenience, the period is fixed at 1 year and the level of forcing can be considerable. We must therefore apply our nonlinear techniques and understanding to the results of numerical simulations. The methodology used in this paper has similarities to the work on phase-resetting maps for kicked oscillators [33]; in our models the kicks occur periodically due to the change between school terms and holidays.

An added problem in understanding the observed case reports of any disease is the effects of noise, which in the disease dynamics can come from two main sources, external fluctuations or internal stochasticity due to the chance occurrence of each event. Stochasticity is epidemiologically important as it allows us to assess the persistence of a disease, with chance events causing the population level of the pathogen to hit zero. Such localised extinctions are a key feature of small populations [9,11,34,35] and understanding their frequency is vital for successful vaccination [36]. Dynamically, stochasticity can force the orbit away from the deterministic attractor leading to transient behaviour playing a far larger role [4]. Section 4 considers the effects of stochasticity on the system, and in particular concentrates on the behaviour of whooping cough, measles and rubella in an attempt to explain the observed dynamics.

2. The basic model and biological paradigm

For simplicity of the mathematics and figures, we shall restrict our attention to the SIR model with constant population size — this reduces the system to two dimensions, as $S + I + R$ is constant. In fact, even the more complex SEIR model [7] which incorporates an incubation period and RAS model [14] which includes age-structure both demonstrate rapid convergence close to a two-dimensional attractor; hence we believe our conclusions are likely to be generic. Traditionally, SIR models have assumed a constant background mortality which affects all individuals equally. For childhood infections however, it is expected that mortality will primarily affect older individuals which will be in the recovered class. This mortality assumption has the added advantage of simplifying the model, although for the parameter regime of interest it does not affect the qualitative dynamics. The basic SIR model can now be written as

$$\frac{\mathrm{d}S}{\mathrm{d}t} = B - \beta SI, \qquad \frac{\mathrm{d}I}{\mathrm{d}t} = \beta SI - gI,$$
$$\frac{\mathrm{d}R}{\mathrm{d}t} = gI - B. \tag{1}$$

Here, S is the proportion of individuals who are susceptible and can therefore catch the disease; I the proportion of individuals who are infectious and can spread the diseases and R are those recovered individuals who have already had the disease (or been successfully vaccinated) so that they are resistant. B represents both the birth and death rates, β is the contact rate which informs us about the spread of the disease and g the rate at which infection is lost (hence g^{-1} is the average infectious period). Throughout we assume that $S + I + R = 1$ and ignore the recovered class.

For any given contact rate β ($> g$), the unforced SIR model (1) has a globally attracting fixed point (for all positive S and I),

$$I^*_\beta = \frac{B}{g}, \qquad S^*_\beta = \frac{g}{\beta},$$

and the Jacobian of this fixed point is

$$J_\beta(S^*, I^*) = \begin{pmatrix} -\beta I^* & -\beta S^* \\ \beta I^* & \beta S^* - g \end{pmatrix} = \begin{pmatrix} -BR_0 & -g \\ BR_0 & 0 \end{pmatrix}.$$

Here $R_0 = \beta/g$ is the basic reproductive ratio and is defined as ‘the average number of secondary cases caused by an infectious individual in a totally susceptible population’ [7]. R_0 is one of the most important epidemiological parameters; only when R_0 is greater than 1 can a disease enter and persist in the population. In general, we expect the birth rate, B, to be small

Table 1
The basic reproductive ratio, R_0, and the infectious period, g^{-1}, for three common childhood diseases in England and Wales (data from [7])[a]

Disease (England and Wales)	R_0	g^{-1} (days)	Natural period (years)
Measles	17	13	2.1
Whooping cough (pertussis)	17	23	2.7
Rubella	7	18	3.7

[a] The natural period of small amplitude perturbations is calculated from the imaginary part of the eigenvalue at the fixed point (with $B = 5.5 \times 10^{-5}$ per day).

compared to the timescale of the epidemic, hence the eigenvalues of the system are complex,

$$\Gamma_\beta = -\frac{BR_0}{2}\left(1 \pm \mathrm{i}\sqrt{\frac{4g}{R_0 B} - 1}\right). \tag{2}$$

The fixed point is therefore always stable and small amplitude perturbations from the fixed point will spiral inwards with a natural frequency determined by the imaginary part of the eigenvalue Γ_β. For three common childhood diseases (measles, whooping cough and rubella) Table 1 gives the basic parameters and this natural period for small oscillations.

In the work that follows, the observed dynamics of these three childhood diseases will be used as a reference (Fig. 1). Measles has been extensively studied in both the modelling [4,13,15,20,36] and time-series literature [1,3,18,19,37,38], and represents one of the most detailed spatio-temporal data sets in ecology. Similar case reports exist for whooping cough, but until recently it had received much less attention [12,17,39]. Despite having comparable values of R_0, measles and whooping cough have very different dynamics [12,39]; any mathematical theory should be able to explain this discrepancy. In contrast, rubella is an epidemiological enigma, with no mechanistic understanding of its dynamical behaviour. The data shows large outbreaks with variable inter-epidemic periods, which has been attributed to chaotic dynamics [16,40]. The aim of this paper therefore is to achieve a comprehensive theory that explains the known behaviour of measles and whooping cough, and to extend the system to model rubella.

The standard SIR equations demonstrate damped oscillations (with periods given in Table 1), however, observations of the case reports of childhood diseases do not show such damping; instead regular cycles are often witnessed (Fig. 1). These periodic epidemics can be captured by introducing term-time forcing into the SIR model. When children are at school, there are assumed to be more interactions between them and thus the term-time contact rate should be larger [18,41]. For simplicity many of the original models assumed that the seasonal forcing could be approximated as a sinusoidal function,

$$\beta(t) = \beta_0(1 + \beta_1 \sin(2\pi t)).$$

As β_1 was varied, a period-doubling route to chaos was observed [15,31], this generated much excitement and prompted many researchers to look for chaos in epidemiological time series [1,3,42]. More recent models, motivated by biological realism, rather than mathematical simplicity, have taken the contact rate to be governed by the school terms,

$$\beta(t) = \beta_0(1 + \beta_1 \mathrm{Term}(t)),$$

where Term is a periodic function which is $+1$ during school terms and -1 during school holidays [13,14] (Table 2 gives the times of terms and holidays used throughout the paper). However, throughout this paper an alternative, and more natural, form will be used,

$$\beta(t) = \beta_0(1 + \beta_1)^{\mathrm{Term}(t)}. \tag{3}$$

Although these two forms are equivalent after re-scaling parameters, the second form is far more convenient as we do not have to place an upper bound

Table 2
Timings of the major school holidays when Term $= -1$, during all other times Term $= +1$[a]

Holiday	Days	Date
Christmas	356–6	21st December–6th January
Easter	100–115	10th–25th April
Summer	200–251	19th July–8th September
Autumn half-term	300–307	27th October–3rd November

[a] The autumn half-term break is included as this is the only short holiday that has an identifiable signature in the England and Wales data.

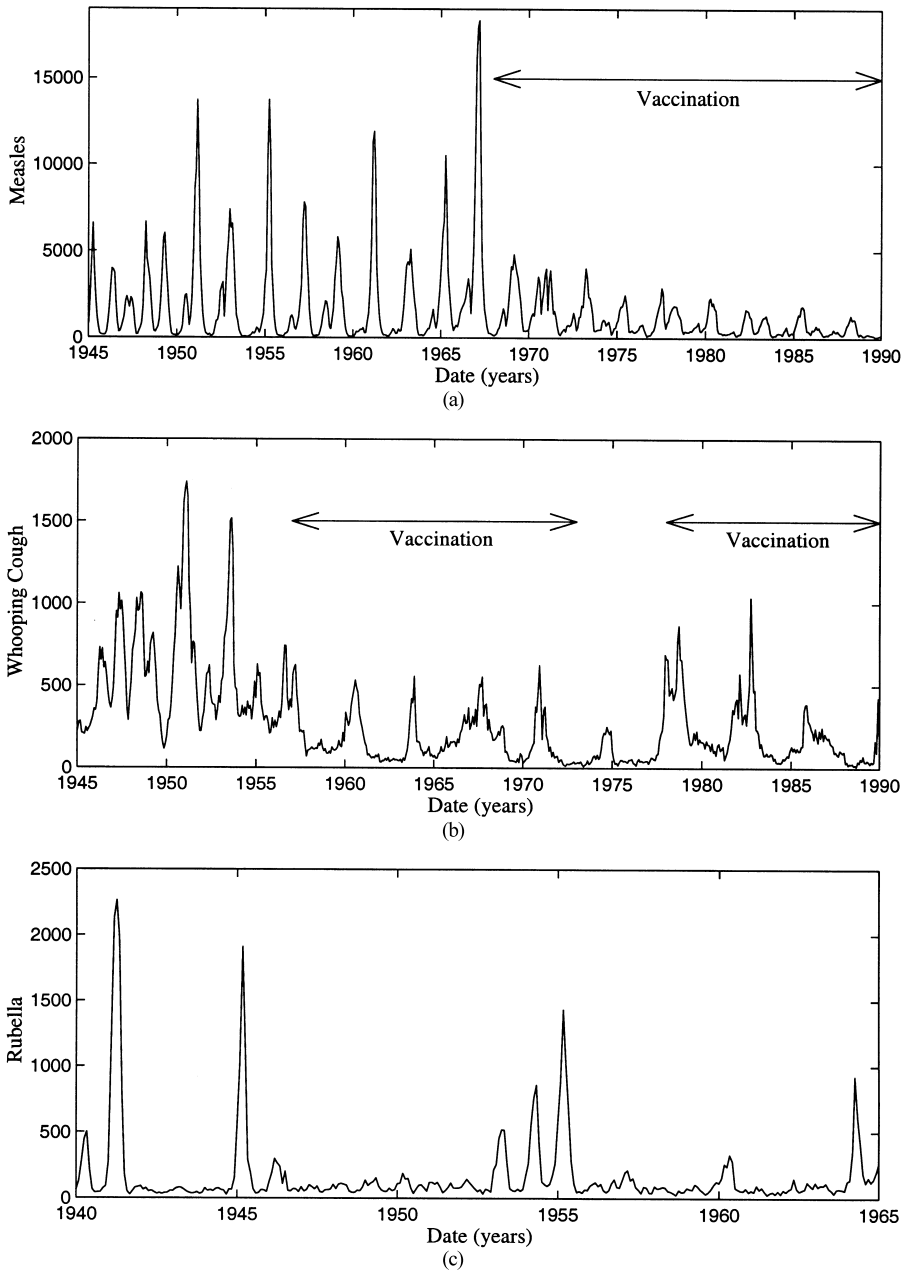

Fig. 1. Time series of the case reports of three childhood diseases in developed countries: (a) measles, (b) whooping cough, (c) rubella. Graphs (a) and (b) are for London, (c) is for Copenhagen. For measles and whooping cough periods of vaccination are indicated.

on β_1. Also, when β is seasonally forced, we find that the basic reproductive ratio, R_0, is given by the long-term geometric average of β/g, so Eq. (3) is the more natural formulation,

$$R_0 = \frac{\beta_0}{g}(1+\beta_1)^{(\text{school days}-\text{holidays})/365} = \frac{\hat{\beta}}{g}.$$

The standard paradigm in epidemiology is that the observed period of the epidemics is due to the

term-time forcing causing the system to resonate close to its natural frequency, although with a period that is an integral multiple of a year. This is not necessarily the case; while it is true that small amounts of random noise will cause the system to resonate near its natural frequency [34], forcing the system with a deterministic annual function can induce far more complex behaviour. The observed epidemics cannot be solely the product of noise, either internally generated or external, as very similar large amplitude epidemics are observed for all population sizes, despite the fact that the relative amount of noise experienced will be very different [43]. This leads us to conclude that the majority of the cyclic behaviour is part of an underlying deterministic pattern.

For the 'binary' type of term-time forcing that is experienced, we can view the system as switching between two fixed point spiral sinks (one for term-time when β is high, another for holidays when β is low). Fig. 2 shows the seasonally forced attractors for measles, whooping cough and rubella; by 'extending' the orbits the switching between the two spiral-sink attractors is clearly visible. The orbits are traced out anti-clockwise, with an abrupt change in direction every time a switch from term-time to holidays (or vice versa) occurs. Using the concept of switching between spiral-sink attractors we are able to consider the behaviour of the forced SIR equations in more analytical detail.

3. Switching between attractors

The concept of switching between term and holiday fixed points shall now be used to consider the dynamics for two very different ranges of seasonality, β_1. When β_1 is small it is possible to perform some rigorous analysis; however, for more realistic amounts of seasonality, we must rely on numerical simulation.

3.1. Small seasonality

When β_1 is small, we can consider the long-term deterministic dynamics to be completely determined by the Jacobians at the fixed points corresponding to the two β values ($J_{\beta_0(1+\beta_1)}$ and $J_{\beta_0/(1+\beta_1)}$). Our model therefore reduces to switching between two near-identical spiral sinks. In this case, irrespective of the natural frequency of the fixed points or the mixture of terms and holidays, the deterministic models will always exhibit annual behaviour (Appendix A).

When the seasonality is small however, the amplitude of the deterministic oscillations will also be small. This in turn means that the deterministic dynamics are far more likely to be swamped by stochastic effects and, as stated earlier, stochastic noise will lead to irregular oscillations close to the natural frequency. Therefore, although we can predict the deterministic behaviour for small forcing, the deterministic approximation is unlikely to be of value for real epidemiological problems. This illustrates the problems that can occur if we use a deterministic analysis to look at a stochastic system.

3.2. Larger seasonality

An increase in the seasonality β_1 means that the fixed points of the two attractors move further apart, the amplitude of the oscillations increases and therefore nonlinear effects play a stronger role. The Jacobians of the two fixed points can therefore no longer be expected to determine the system's long-term dynamics. Without the nonlinear effects only two scenarios are possible, either the annual cycle remains globally stable or ever growing oscillations are observed [44]. Therefore, the presence of nonlinearities is vital if we are to obtain the rich array of observed dynamics.

We now consider the deterministic periodicity of childhood diseases, when a realistic amount of term-time forcing is introduced. Although the basic reproductive ratio and infectious period can be measured directly, the magnitude of seasonal forcing, β_1, is more difficult. For many years it has become the standard approach to calculate a bifurcation diagram for changes in β_1 [15]. Although this is a good approach when considering a disease in isolation, the seasonality parameters for all childhood diseases have the same underlying cause — the opening and closing of schools — and therefore should be related.

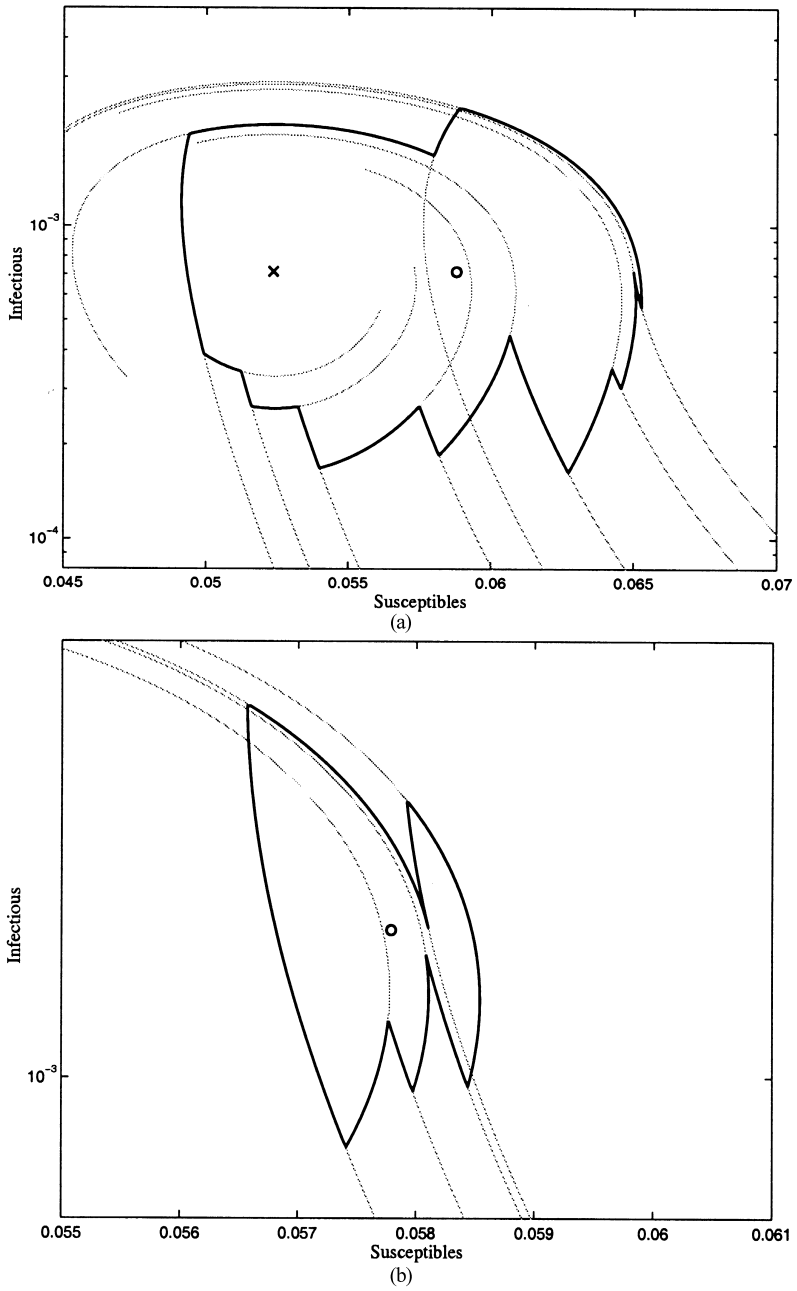

Fig. 2. The long-term attractors for measles (graph (a)), whooping cough (graph (b)) and rubella (graph (c)). The solid black lines give the deterministic attractors of the forced system; the grey lines show the continuation of the orbits if the switch between term and holidays did not occur. These continuation lines clearly show that the attractor is switching between two spiral-sink orbits. The fixed point of the term-time attractor is shown as a cross, and the fixed point for the unforced system is shown as a circle; the holiday-time fixed points (and the term-time fixed point for whooping cough) lie outside the scale of the graphs. For rubella, we show both the 1 and 5-year attractors.

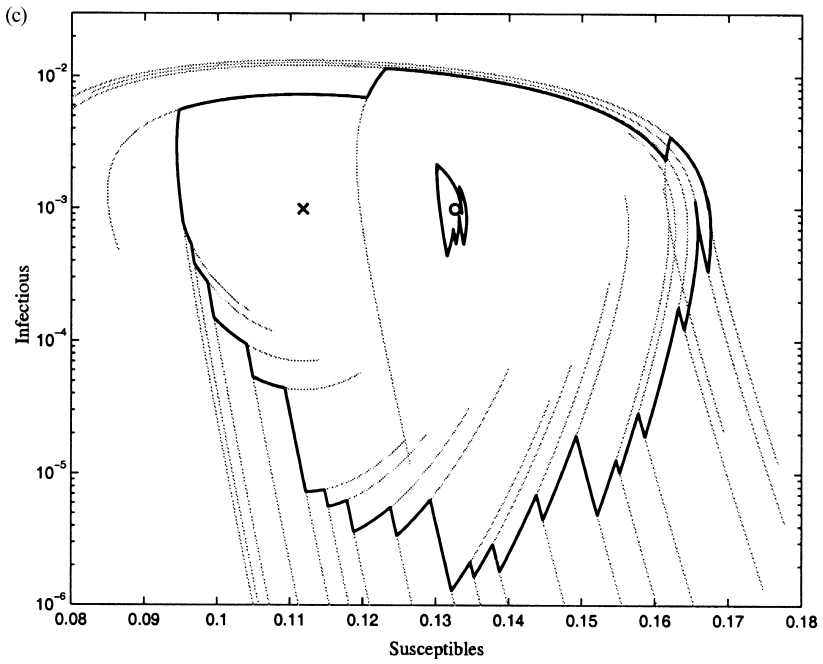

Fig. 2. (*Continued*).

The value of β_1 can be approximated by considering directly the mixing between susceptible and infectious school children of the same age. From the differential equations (1), and ignoring any heterogeneity in transmission, we find the proportion of the population of age A that are susceptible or infectious is given by [7]

$$\frac{\mathrm{d}S}{\mathrm{d}A} = -\beta S(A) I^* \Rightarrow S(A) = \exp(-ABR_0)$$
$$\Rightarrow I(A) = \frac{1}{g}\frac{\mathrm{d}S}{\mathrm{d}A} = \frac{BR_0}{g}\exp(-ABR_0).$$

It will be assumed that the extra mixing during school terms comes from the greater interaction between children of the same age. Therefore, β_1 can be approximated by

$$\beta_1 \propto \frac{\int_{\text{school ages}} S(A) I(A)\,\mathrm{d}A}{\int_0^\infty S(A)\,\mathrm{d}A \int_0^\infty I(A)\,\mathrm{d}A}$$
$$\propto BR_0[\exp(-2A_S BR_0) - \exp(-2A_L BR_0)], \quad (4)$$

where A_S and A_L are the ages a child starts and leaves school. From extensive computer simulation it has been found that $\beta_1 \approx 0.25$ gives a good approximations to the biennial measles dynamics [13]; this allows us to calculate the proportionality constant. Table 3 gives the values of β_0 and β_1 that are used in all subsequent calculations. It should be noticed that due to the higher mean age of infection, rubella experiences far larger levels of seasonality than measles or whooping cough.

Using a birth rate of $B = 5.5 \times 10^{-5}$ per day, and with β_1 given by Eq. (4), the SIR equations (1) can be solved numerically for the term-time pattern from England and Wales. Fig. 3 shows the calculated period for a range of basic reproductive ratios, R_0, and infectious periods, g^{-1}. Large R_0 or large infectious periods favour annual dynamics, whereas smaller R_0 and

Table 3
The contact rate, β_0, and seasonality, β_1, for three common childhood diseases in England and Wales[a]

Disease (England and Wales)	β_0	β_1	Period (years)
Measles	1.175	0.25	2
Whooping cough	0.664	0.25	1
Rubella	0.311	0.5981	1 and 5

[a]The period of the forced oscillations was calculated by numerical integration to find the attractor (see Fig. 3).

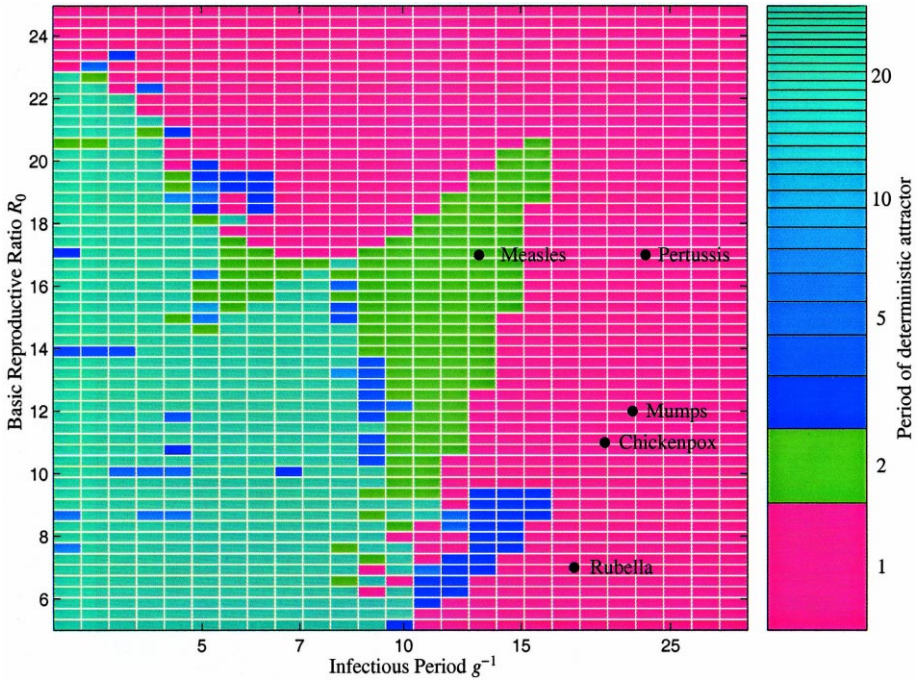

Fig. 3. The period of the deterministic attractor of the SIR model (1) starting from the unforced fixed point $(S^*_{\hat{\beta}}, I^*_{\hat{\beta}})$ for a range of infectious periods and reproductive ratios — notice that the x-axis is on a logarithmic scale. The sites are colour coded, red for annual, green for biennial, and blue for longer orbits; the darkest blues correspond to 3-year cycles and the lightest blues represent chaos or orbits with periods of more than 100 years. For reference, the parameters of five childhood diseases, measles, whooping cough, rubella, mumps and chickenpox are shown.

smaller infectious periods lead to long-period oscillations or chaos. The deterministic period can also be compared to the eigenvalues of the unforced system, $\Gamma_{\hat{\beta}}$. The long-period (chaotic) regime corresponds to the eigenvalues having small negative real parts, so that convergence is slow, and large imaginary parts, so the unforced system would possess rapid oscillations. Both of these conditions mean that during a change from term-time to holidays and back to term-time the system can experience strong nonlinear behaviour; which in turn leads to the complex dynamics.

Looking at the three childhood diseases in particular, the deterministic model predicts that whooping cough (Fig. 2b), has annual dynamics — simulations indicate that these annual cycles are globally attracting. Measles parameters exists within a triangle of biennial behaviour, hence its 2-year cycles (Fig. 2a) should be robust to moderate changes in birth rate, mixing or other parameters. This agrees well with the observed pattern in developed countries before vaccination. Finally, although the parameters for rubella show annual dynamics when starting at the unforced fixed point $(S^*_{\hat{\beta}}, I^*_{\hat{\beta}})$, it is fairly close to the longer-period regime and more extensive simulations have shown that there exists a second coexisting attractor with 5-year period (Fig. 2c).

Three factors may disrupt this picture: the first is that some diseases such as whooping cough are not fully captured by the SIR model due to waning immunity — however this phenomenon can generally be absorbed into the parameters without radically changing the nature of the attractor [39,45]. Another complication is the approximation of β_1; this assumed homogeneous mixing to find the susceptibility profile whereas more realistic age-structured models [6,7,14] would provide a better estimation for the seasonality. How-

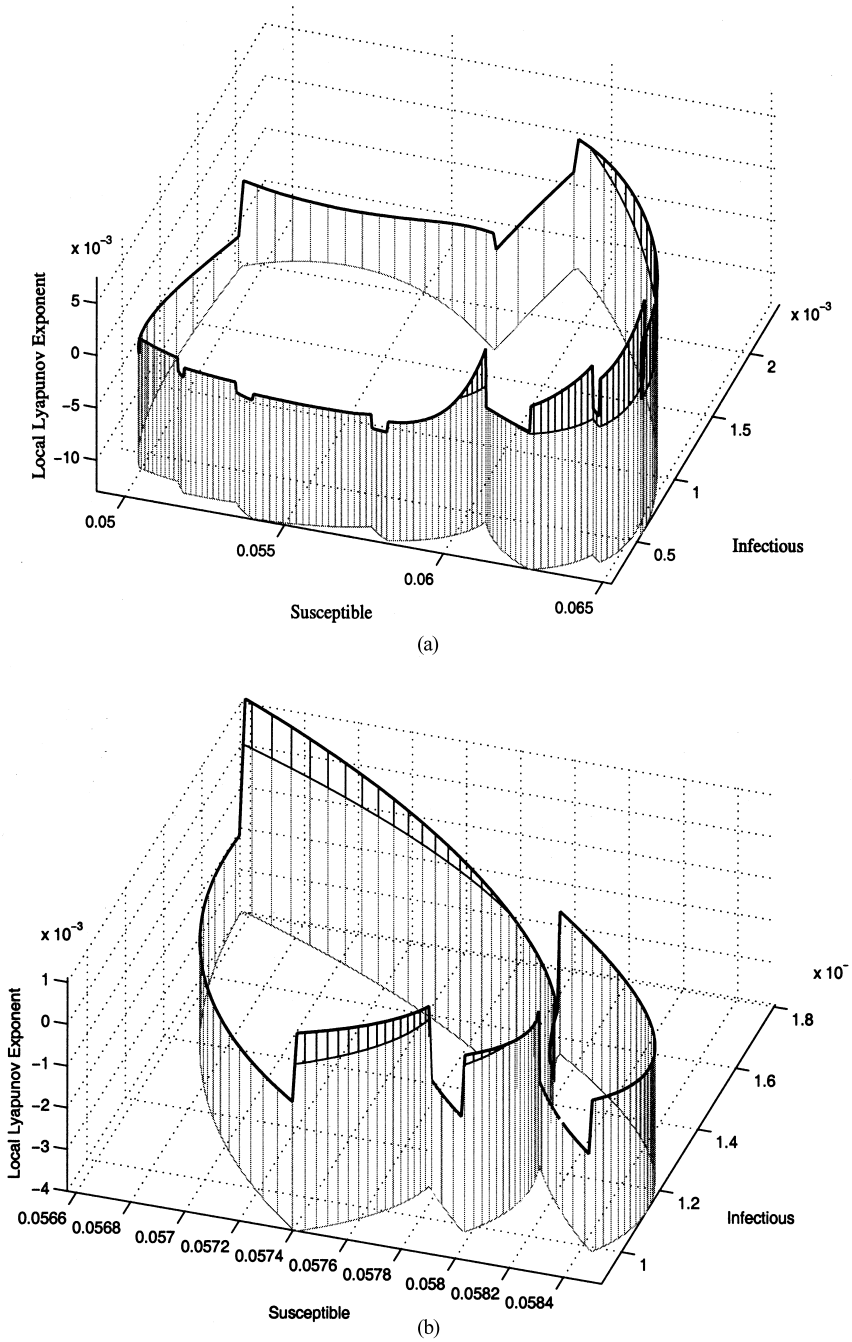

Fig. 4. Local Lyapunov exponents at various points around the deterministic attractor for measles (graph (a)) and whooping cough (graph (b)). The value of the Lyapunov exponent is shown with a thick black line; the height of the Lyapunov exponent above zero (where the attractor is locally expanding) is shaded black.

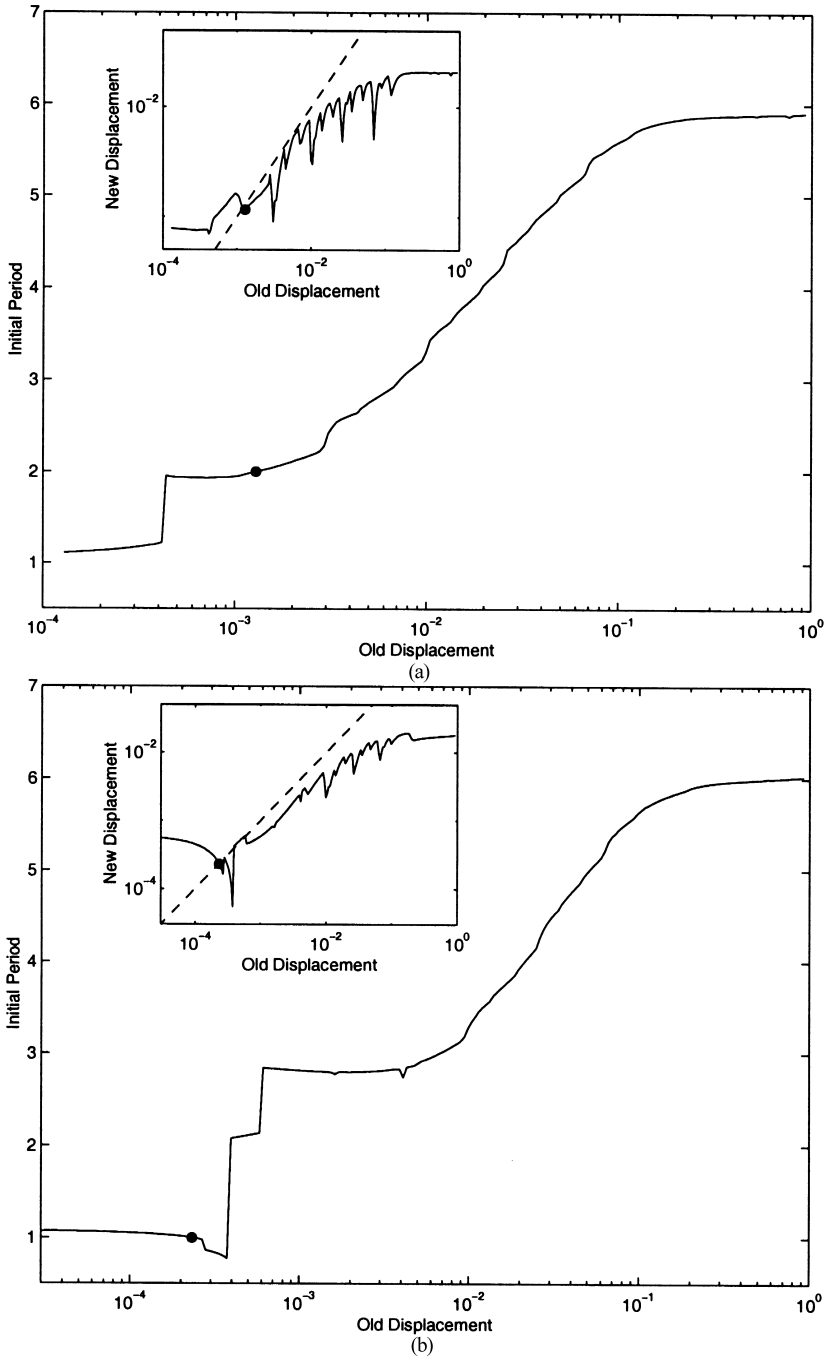

Fig. 5. For a given displacement D from the unforced fixed point $(S^*_{\hat{\beta}}, I^*_{\hat{\beta}})$, the initial period, $T(D)$, and the subsequent displacement $F(D)$ (inset). Graph (a) is for measles, graph (b) is for whooping cough and graph (c) is for rubella.

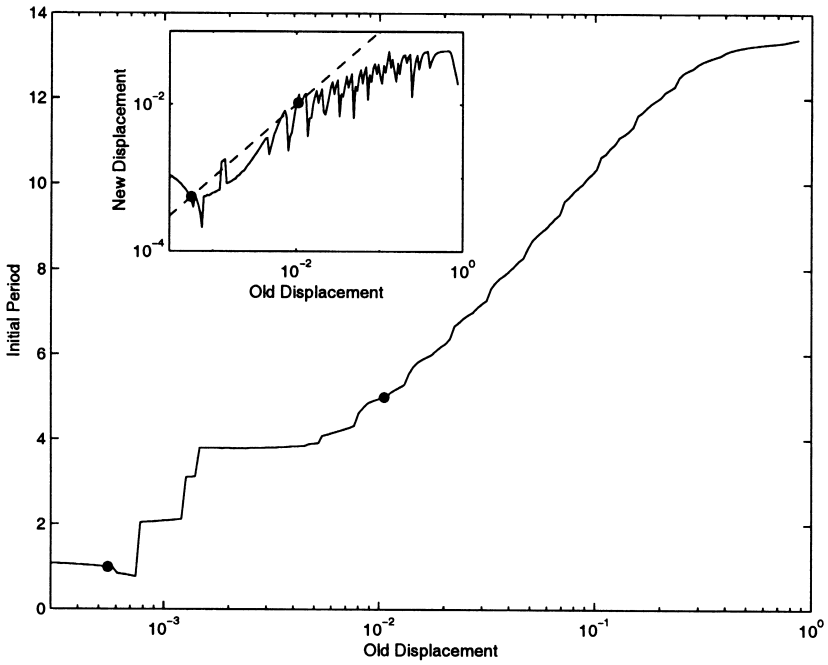

(c)

Fig. 5. (*Continued*).

ever, by far the largest missing ingredient is stochasticity — demographic noise may push orbits away from the deterministic attractor and transient behaviour will play a more important role in the long-term dynamics. In the next section, concentrating primarily on measles, whooping cough and rubella, we consider the periodic nature of these perturbed cycles.

4. Stochasticity and large deviations

In order to explain why noise has a greater effect on the dynamics of whooping cough than measles we shall at first consider the stability of the attractor; the usual method of doing this is to calculate the Lyapunov exponents. Fig. 4 shows the local Lyapunov exponents around the orbit (see Appendix B for the method of calculation). It is clear that both attractors have some regions where the Lyapunov exponent is positive and hence perturbations grow. However, measles actually has more of these unstable regions and a less negative global Lyapunov exponent, so locally the measles attractor is less stable. The Lyapunov exponents therefore fail to explain the observed effects of noise, predicting that measles dynamics should be more sensitive to perturbations than whooping cough. This failure is presumably because Lyapunov exponents only measure the local linear behaviour around the attractor, whereas the observed stochastic dynamics is strongly influenced by large deviations away from the attractor and hence nonlinear behaviour. In this section therefore, we consider the transient behaviour of the seasonally forced model for a range of perturbations.

Starting from the fixed point of the unforced system $(S^*_{\hat\beta}, I^*_{\hat\beta})$ (where $\hat\beta = R_0 g$), we apply a positive displacement D to the density of infectious individuals,

$$S(t_0) = S^*_{\hat\beta}, \qquad I(t_0) = I^*_{\hat\beta} + D \tag{5}$$

and find the time for a single revolution when seasonal forcing is included. The initial time, t_0, is chosen such that the seasonally forced attractor conforms to Eq. (5). Due to the strengthening role of nonlinearities, the unforced model rotates slower the further the system is from the fixed point attractor and this general trend

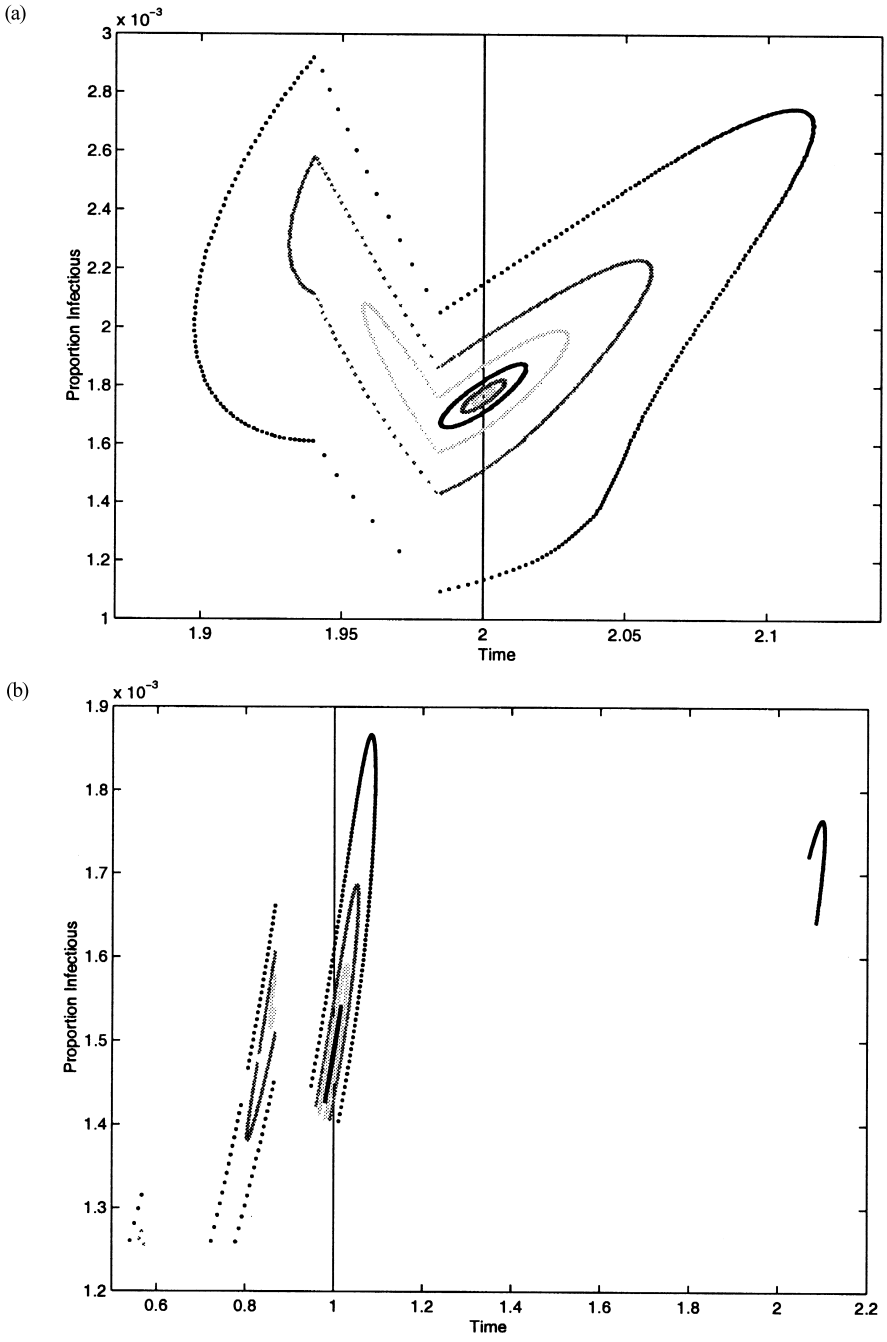

Fig. 6. For a range of circular perturbations about one point on the deterministic attractor, the displacement D above the fixed point $(S^*_{\hat{\beta}}, I^*_{\hat{\beta}})$, and the time T taken to get to that point. Graph (a) is for measles, graph (b) is for whooping cough and graph (c) is for rubella (circles around the annual attractor are grey, those around the 5-year cycle are in black). More precisely, T is the time taken until the point crosses the line $S = S^*_{\hat{\beta}}$ (with $I > I^*_{\hat{\beta}}$) for the first time if we start with $S(t_0) \geq S^*_{\hat{\beta}}$ or for the second time if we start with $S(t_0) < S^*_{\hat{\beta}}$. Hence the points of the circle have completed approximately one revolution. The maximum circle used had a radius equal to the standard deviation around the deterministic orbit.

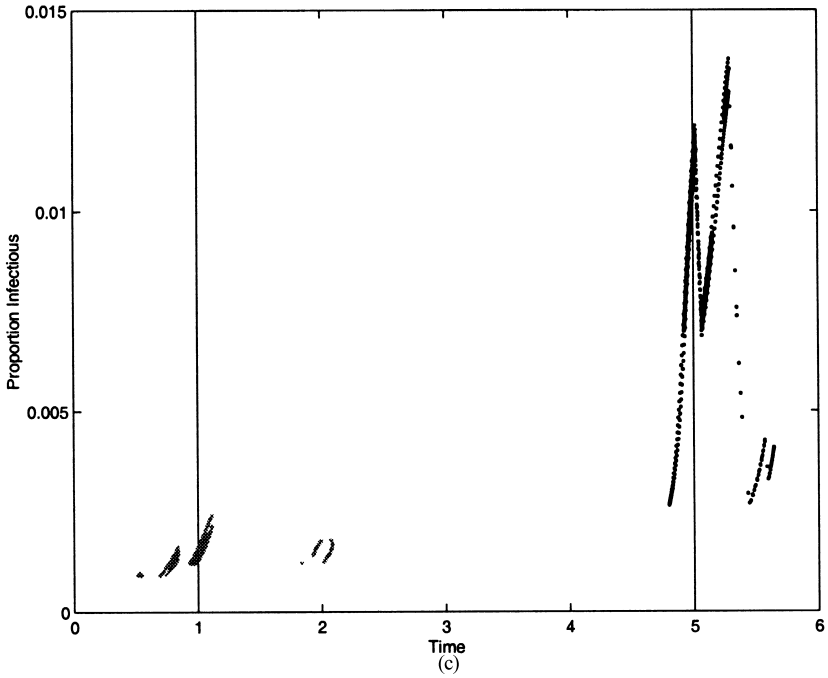

Fig. 6. (*Continued*).

is expected to hold for the forced model. For a given displacement, D, the initial period of one revolution, $T(D)$, is defined as,

$$T(D) = \inf\{t > 0 : S(t_0+t)=S^*_{\hat{\beta}} \text{ and } I(t_0 + t) > I^*_{\hat{\beta}}\}.$$

This value of T therefore corresponds to a transient inter-epidemic period. Fig. 5 shows this process for the three diseases, measles, whooping cough and rubella, which display very different behaviour; the large dot gives the displacement of the stable deterministic attractor. For very small displacements (close to the unforced fixed point) the initial period of rotation is close to annual for all three diseases. We note that all graphs exhibit discrete jumps in period (e.g. from 1 to 2 years in measles and from 1 to 2 and 2 to 3 years for whooping cough), these jumps are due to the way in which revolutions are counted and are closely associated with a topological change in the orbit.

Something akin to a Poincaré return map for the displacement, D, can now be found for each complete cycle,

$$D' = F(D) = I(T(D)) - I^*_{\hat{\beta}},$$

which is shown in the inset graphs of Fig. 5. This is not a true Poincaré return map as we would need to know both the time and the displacement to predict the future dynamics. However, by looking at the 'new displacement' (D') after one cycle, and we can observe whether orbits are expanding or contracting and hence obtain some intuition about the dynamics. Note that for a displacement D to be a fixed point of the full seasonally forced system, we require it to be a fixed point of the return map F and for the period $T(D)$ to be an integral multiple of 1 year.

The return map $F(D)$ and the initial period $T(D)$ (Fig. 5) can now be used to understand the observed dynamics of measles, whooping cough and rubella (Fig. 1). For the measles parameters (Fig. 5a), the seasonally forced attractor is the only fixed point of F and is locally stable, and at this point $T(D)$ has a plateau such that the displacement, D, has only a gradual effect on the period. Therefore, small stochastic perturbations to the measles attractor are likely to have little effect on either the period or amplitude of the epidemics. This demonstrates why the simple determin-

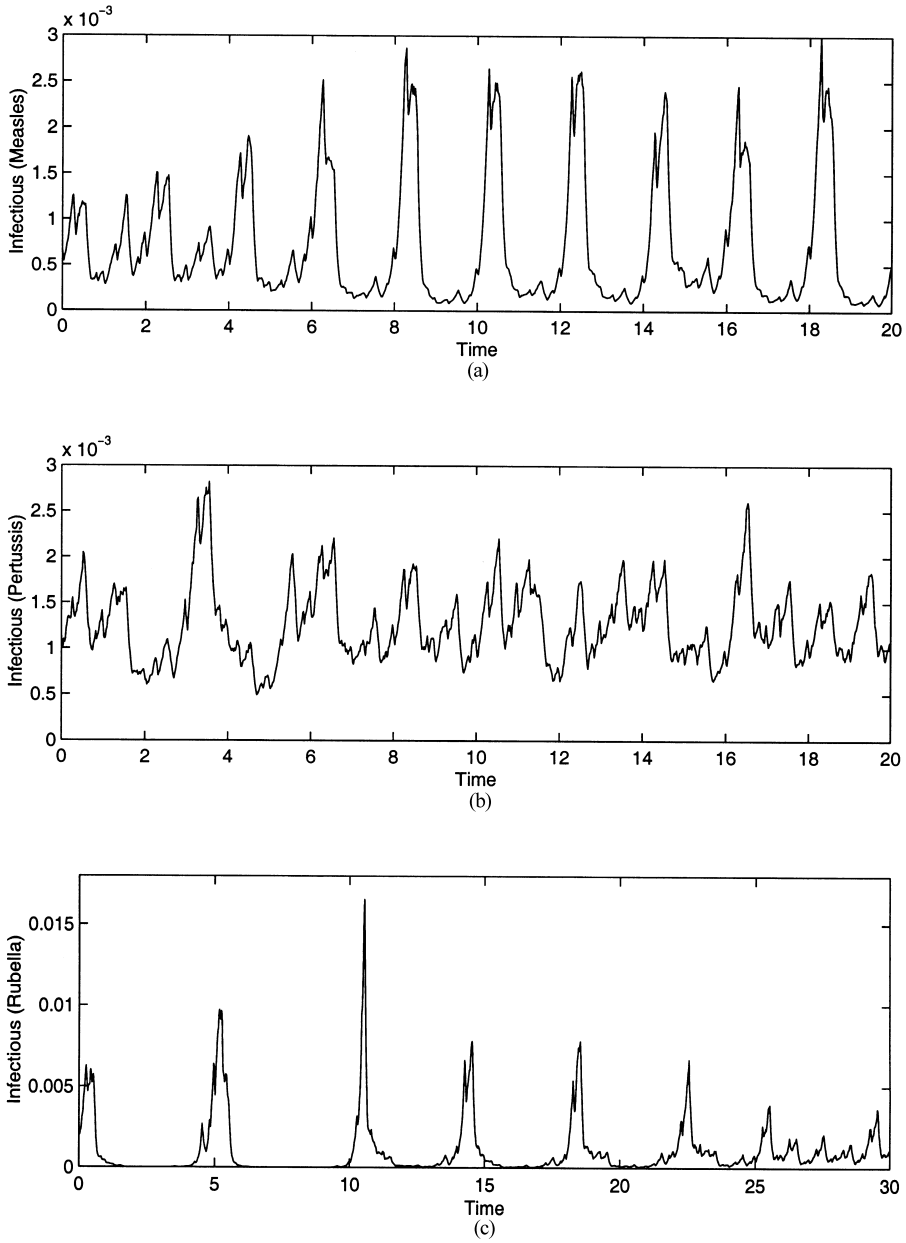

Fig. 7. The dynamics of measles (graph (a)), whooping cough (graph (b)) and rubella (graph (c)) before vaccination from the seasonally forced SIR model together with 1% multiplicative noise. The graphs show a typical section of the simulation, once transient behaviour has died out.

istic models for measles have been so successful at predicting the qualitative behaviour.

For whooping cough the picture is very different, small positive perturbations away from the deterministic attractor can give rise to biennial epidemics and slightly larger perturbations move the system into a plateau of triennial oscillations. The return map for whooping cough also shows more complex behaviour

than its measles counterpart. Therefore, whooping cough epidemics should be more prone to stochastic effects, which may take the dynamics into regions of biennial or even triennial behaviour.

Finally, for rubella there exist two stable attractors with periods of 1 and 5 years, respectively. From the return map, it is clear that other fixed points of the map also exist — although these correspond to non-integer periods and are therefore not associated with an attractor of the full system. The annual attractor has a larger basin of attraction and is thus more robust to perturbations than the 5-year attractor, although the log-scaling on the graph overemphasises this aspect. However, the larger amplitude 5-year cycles are more likely to occur on introduction of the disease or after a stochastic extinction and subsequent reintroduction. Therefore, rubella can be expected to show a mixture of 1 and 5-year periods, very much akin to the observed pattern in the Copenhagen data.

An alternative method of examining the response of the disease models to large perturbations is shown in Fig. 6. We start with a set of concentric circles, centred about the point on the deterministic attractor $(S(t_0) = S^*_{\hat{\beta}}, I(t_0) > I^*_{\hat{\beta}})$. Each point in these circles is then iterated forward and we again record the displacement D and the time T taken for the point to complete approximately one revolution. In Fig. 6a for measles it is clear that the circles undergo a small amount of stretching, with the abrupt change to the circles due to nearby points moving in opposite directions when the switch between attractors occurs. For whooping cough (Fig. 6b) the stretching is far more violent, and the time taken for a revolution varies dramatically from 6 months to 2 years. Therefore, while very small circles contract more rapidly in the whooping cough model than for measles (as predicted by the Lyapunov exponent), large perturbations undergo far more stretching and variation of period.

For rubella, we placed concentric circles for both attractors (Fig. 6c). While the circles associated with the 5-year cycle undergo more stretching than the 1-year circles, their period is much more constrained. Perturbations to the 1-year attractor can lead to multi-annual cycles which eventually converge back to the annual attractor. In contrast, for the less robust 5-year attractor even large perturbations always give rise to transient dynamics with a 5–6-year inter-epidemic period, so in the short-term the qualitative behaviour of the cycle is maintained.

We can test the understanding we have gained about the stochastic system by considering the behaviour of the SIR model for measles, whooping cough and rubella subject to a small amount of multiplicative noise (Fig. 7). Even in the presence of noise, measles dynamics shows predominately biennial cycles as predicted by the deterministic model, although a short period of more annual behaviour can be seen in years 0–3. For whooping cough — in contract to the deterministic model — the presence of noise generates a complex mixture of multi-annual cycles. The time-series of both the measles and whooping cough are a good characterisation of the reported cases from England and Wales. Finally for rubella, we observe the transition from 5-year cycles, through 4-year cycles (which are not seen in the deterministic model, but correspond to a plateau in Fig. 5c) to 1-year outbreaks. This model shows frequent noise-induced transition between these three patterns, and therefore may explain the complex dynamics that have been observed.

5. Conclusion

The SIR model (and other related models of infectious diseases) are amongst the simplest and yet most accurate of all biological models [5,8,9]. The rapid mixing within a large human population means that the mass-action assumption for disease transmission is a good approximation, and the presence of this single nonlinearity means that these models are well suited for detailed mathematical study [4,13,16]. The dynamical study of disease behaviour has benefited both subjects, pushing mathematics into the study of novel and more complex situations and providing epidemiologists with the tools and framework to understand their observations.

The dynamics of the seasonally forced SIR model is best considered as switching between two stable spiral sinks. This idea of switching between two at-

tractors, one for the term-time β and another for the holiday β, could easily be extended to more complex disease models and other biological systems where there are distinct seasonal changes. Although throughout this paper we have used a single pattern of holidays and school terms, extensive simulations have shown that in general the qualitative features and methodologies hold for a wide range of holiday patterns although the precise dynamics may vary [6].

We have shown analytically that very small differences between terms and holidays (as measured by β_1) always lead to annual dynamics. In fact we believe that annual deterministic attractors are primarily the result of relatively localised dynamics such that nonlinearities do not play an important role. It is interesting to note that rapid switching between attractors (relative to the disease dynamics) means that the orbit does not have the opportunity to move far enough to experience any nonlinearities. Therefore, only small oscillations at the same period as the forcing will be observed. This explains why weekends can be ignored in disease modelling; despite the fact that they may cause large changes in the contact parameter β, these changes are so short that they never interact with the nonlinearities of the system.

When the seasonality is larger, the dynamics become more complex (Figs. 2 and 3). Increasing seasonality leads to the standard period-doubling bifurcations for measles and many other disease parameters [13,15]. However, here we have taken a different approach, by assuming that all children experience the same holidays and school terms, we have considered how the deterministic period varies with the basic disease parameters R_0 and g. The deterministic attractor is annual when either R_0 or the infection period (g^{-1}) is large. This corresponds to greater stability of the fixed points or slower rotation about the fixed point, both of which lead to the orbit experiencing fewer nonlinearities due to switching. Correspondingly, short infectious periods and small R_0 lead to longer cycles or chaotic dynamics.

When comparing theory to observations it is important to contrast the period of the deterministic attractor with the observed frequency of epidemics. For example, many large period attractors will develop a major epidemic every year, with only small differences between subsequent years; this has been found to occur when R_0 is large and the infectious period is small. Obviously such dynamics have a very large annual component and only a weak signature of higher periods should be observed in case report data. In contrast the initial period calculated in Section 5, generally measures the period between major epidemics and therefore compares more favourably with epidemiological intuition and imprecise observations.

The observed dynamics, both from simulations and from case reports in England and Wales or Copenhagen, are a mixture of the deterministic behaviour together with stochastic effects [46]. By considering the two maps, F and T, for the initial period and subsequent displacement, we can assess the likely effects of stochasticity. The return map clearly shows that the period of whooping cough is far more susceptible to stochastic perturbations than measles. This explains why the majority of communities in England and Wales (Type I and II communities in the nomenclature of Bartlett [34]) show biennial measles dynamics, yet only the largest cities display bouts of annual dynamics for whooping cough. Rubella possesses two stable attractors, with periods of 1 and 5 years, respectively. Rubella should therefore show a mixture of periodic cycles, from annual to around 5 years; while this is consistent with the data for Copenhagen, more research and data are needed to fully understand this important disease.

In conclusion, the dynamics of childhood diseases subject to seasonal forcing is far more complex than it would first appear. By concentrating on the behaviour of measles, where simple explanations and observations coincide, earlier epidemiological theory has overlooked many of the complexities that are present. This work has made a preliminary investigation of the interplay between seasonality, deterministic dynamics and stochasticity, linking biologically interesting problems with a more mathematical understanding of the behaviour of models. Biologically realistic models offer a wealth of nonlinear problems to motivate mathematical study, and a strong inter-disciplinary approach will have benefits for both subjects.

Acknowledgements

This research was supported by the Royal Society (MJK and PR) and the Wellcome Trust (BTG). We wish to thank Robert MacKay for his help, as well as Colin Sparrow for his useful comments on this manuscript.

Appendix A

Theorem. *When the difference between term-time and holidays is small* ($\beta_1 \ll 1$) *for any annual patterns of terms and holidays there exists a unique stable globally attracting annual cycle.*

Let us define β^+ and β^- to be the term-time and holiday contact rates,

$$\beta^+ = \beta_0(1+\beta_1), \qquad \beta^- = \frac{\beta_0}{1+\beta_1} \leq \beta_0(1-\beta_1).$$

When β_1 is small, the term-time and holiday fixed points will be close and have very similar Jacobians. Therefore when an orbit is far from the fixed point, the effects of switching between attractors will be negligible and orbits will spiral in towards the attractors as if they were a single point. In particular, for any positive ε, we can find a β_1 such that all orbits converge to within ε of the unforced fixed point $(S^*_{\hat{\beta}}, I^*_{\hat{\beta}})$.

Once within this ε ball, we can assume that all orbits are close enough to the fixed points that nonlinearities can be ignored and the dynamics are given purely by the Jacobian. Hence, for small β_1, our problem reduces to switching between two near-identical spiral sinks. Now instead of viewing the system as switching between two attractors with separated fixed points, we consider a single fixed point and repeatedly displace the orbit.

We decompose the orbit into two operations, periods on the attractor ($A^{\pm}$) followed by displacements ($D^{\pm}$). Given a periodic sequence of holidays and school terms, of lengths $(h_1, h_2, \ldots, h_n)$ and $(t_1, t_2, \ldots, t_n)$, the dynamics of 1 year are given by,

$$Y = A^+_{t_n} D^+ A^-_{h_n} D^- A^+_{t_{n-1}} D^+ A^-_{h_{n-1}} D^- \cdots A^+_{t_1} D^+ A^-_{h_1} D^-,$$

where

$$D^{\pm}(x, y) = (x \pm \beta_1, y)$$

and as the orbits have converged to within $\varepsilon \ll 1$ of the fixed points, the A can be considered as linear functions.

It is clear to see that Y is a linear function, because it is a composite of linear functions, hence there exists a unique annual cycle starting at (x^*, y^*) such that,

$$Y(x^*, y^*) = (x^*, y^*).$$

Due to the uniqueness condition, (x^*, y^*) must be the only solution to orbits with n-year cycles. Therefore, we conclude that for small β_1 there only exists a single annual period orbit.

As this temporally forced orbit lies arbitrarily close to the stable fixed points, it must be described by a similar Jacobian and therefore have similar stability properties.

Appendix B

The calculation of the local and global Lyapunov exponents around the deterministic attractor is based on the time-series techniques of Wilson and Rand [47]. Given a set of parameters $\underline{x}$, we suppose that our dynamics are given by,

$$\frac{\mathrm{d}\underline{x}}{\mathrm{d}t} = f(\underline{x}, t).$$

The simplest way to calculate the local Lyapunov exponent is to find the maximum eigenvalue of the Jacobian of f at each point on the attractor, however this does not take into account the contraction experienced by this eigenvector at nearby points on the attractor. We therefore allow the direction of maximal expansion, $\underline{z}$, to evolve around the orbit. Define z as,

$$\frac{\mathrm{d}\underline{z}_i}{\mathrm{d}t} = (J_{f(\underline{x},t)}\underline{z})_i - z_i(J_{f(\underline{x},t)}\underline{z}) \cdot \underline{z}, \quad \|\underline{z}\| = 1,$$

where $J_{f(\underline{x},t)}$ is the Jacobian of f at the point $\underline{x}$ at time t. The local Lyapunov exponent can then be defined as,

$$L(\underline{x}(t), t) = (J_{f(\underline{x},t)}\underline{z}) \cdot \underline{z},$$

which is the expansion in the $\underline{z}$ direction. The global Lyapunov exponent is defined as the average of the local exponents around the attractor,

$$L_{\mathrm{G}} = \frac{1}{T}\int_0^T L(\underline{x}(t), t)\,\mathrm{d}t.$$

References

[1] W.M. Schaffer, M. Kot, Nearly one-dimensional dynamics in an epidemic, J. Theor. Biol. 112 (1985) 403–427.

[2] L.F. Olsen, G.L. Truty, W.M. Schaffer, Oscillations and chaos in epidemics: a nonlinear dynamic study of six childhood diseases in Copenhagen, Denmark, Theor. Popul. Biol. 33 (1986) 344–370.

[3] G. Sugihara, B.T. Grenfell, R.M. May, Distinguishing error from chaos in ecological time series, Philos. Trans. Roy. Soc. Lond. B 330 (1990) 235–251.

[4] D.A. Rand, H.B. Wilson, Chaotic stochasticity — a ubiquitous source of unpredictability in epidemics, Proc. Roy. Soc. Lond. B 246 (1991) 179–184.

[5] R.M. May, R.M. Anderson, Population biology of infectious diseases, part II, Nature 280 (1979) 455–461.

[6] D. Schenzle, An age-structured model of pre- and post-vaccination measles transmission, IMA J. Math. Appl. Med. Biol. 1 (1984) 169–191.

[7] R.M. Anderson, R.M. May, Infectious Diseases of Humans, Oxford University Press, Oxford, 1992.

[8] D. Mollison, V. Isham, B. Grenfell, Epidemics: models and data, J. Roy. Stat. Soc. A 157 (1993) 115–149.

[9] B.T. Grenfell, B.M. Bolker, A. Kleczkowski, Seasonality and extinction in chaotic metapopulations, Proc. Roy. Soc. Lond. B 259 (1995) 97–103.

[10] N.M. Ferguson, D.J. Nokes, R.M. Anderson, Dynamical complexity in age-structured models of the transmission of measles virus, Math. BioSci. 138 (1996) 101–130.

[11] M.J. Keeling, B.T. Grenfell, Disease extinction and community size: modeling the persistence of measles, Science 275 (1997) 65–67.

[12] P. Rohani, D.J.D. Earn, B.T. Grenfell, Opposite patterns of synchrony: in sympatric disease metapopulations, Science 286 (1999) 968–971.

[13] D.J.D. Earn, P. Rohani, B.M. Bolker, B.T. Grenfell, A simple model for complex dynamical transitions in epidemics, Science 287 (2000) 667–670.

[14] B.M. Bolker, Chaos and complexity in measles models: a comparative numerical study, IMA J. Math. Appl. Med. Biol. 10 (1993) 83–95.

[15] J.L. Aron, I.B. Schwartz, Seasonality and period-doubling bifurcations in an epidemic model, J. Theor. Biol. 110 (1984) 665–679.

[16] L.F. Olsen, W.M. Schaffer, Chaos versus noisy periodicity: alternative hypotheses for childhood epidemics, Science 249 (1990) 499–504.

[17] P. Rohani, D.J. Earn, B. Finkenstädt, B.T. Grenfell, Population dynamic interference among childhood diseases, Proc. Roy. Soc. Lond. B 265 (1998) 2033–2041.

[18] P.E.M. Fine, J.A. Clarkson, Measles in England and Wales I: an analysis of factors underlying seasonal patterns, Int. J. Epidemiol. 11 (1982) 5–14.

[19] B. Finkenstädt, B. Grenfell, Empirical determinants of measles metapopulation dynamics in England and Wales, Proc. Roy. Soc. Lond. B 265 (1998) 211–220.

[20] I.B. Schwartz, Multiple recurrent outbreaks and predictability in seasonally forced nonlinear epidemic models, J. Math. Biol. 18 (1985) 233–253.

[21] K. Tomita, Chaotic response of nonlinear oscillators, Phys. Rep. 86 (1982) 113–167.

[22] J. Guckenheimer, P. Holmes, Nonlinear Oscillations, Dynamical Systems and Bifurcations of Vector Fields, Springer, New York, 1983.

[23] A.F. Vakakis, C. Cetinkaya, Analytic evaluation of period responses of a forced nonlinear oscillator, Nonlinear Dyn. 7 (1995) 37–51.

[24] K. Ullmann, I.L. Caldas, Transitions in the parameter space of a periodically forced dissipative system, Chaos Solitons Fractals 7 (1996) 1913–1921.

[25] B. Barnes, R. Grimshaw, Numerical studies of the periodically forced Bonhoeffer vanderPol system, Int. J. Bifurc. Chaos 7 (1997) 2653–2689.

[26] J.H. Li, K.F. He, Z.Q. Huang, Time-correlation function for periodically forced nonlinear stochastic system, Commun. Theor. Phys. 30 (1998) 397–404.

[27] K. Aihara, G. Matsumoto, Y. Ikegaya, Period and non-periodic responses of a periodically forced Hodgkin–Huxley oscillator, J. Theor. Biol. 109 (1984) 249–269.

[28] L. Glass, M.R. Guevara, J. Belair, A. Shrier, Global bifurcations of a periodically forced biological oscillator, Phys. Rev. A 29 (1984) 1348–1357.

[29] J.P. Keener, L. Glass, Global bifurcations of a periodically forced nonlinear oscillator, J. Math. Biol. 21 (1984) 175–190.

[30] M.Z. Ding, J.A.S. Kelso, Phase-resetting map and the dynamics of quasi-periodically forced biological oscillators, Int. J. Bifurc. Chaos 4 (1994) 553–567.

[31] P. Glendinning, L.P. Perry, Melnikov analysis of chaos in a simple epidemiological model, J. Math. Biol. 35 (1997) 359–373.

[32] S.M. Henson, Multiple attractors and resonance in periodically forced population models, Physica D 140 (2000) 33–49.

[33] R.S. MacKay, Transition of the phase-resetting map for kicked oscillators, Physica D 52 (1991) 266–354.

[34] M.S. Bartlett, Measles periodicity and community size, J. Roy. Stat. Soc. A 120 (1957) 48–70.

[35] B. Grenfell, J. Harwood, (Meta)population dynamics of infectious diseases, TREE 12 (1997) 395–399.

[36] M.J. Keeling, Modelling the persistence of measles, Trends MicroBiol. 5 (1997) 513–518.

[37] B.T. Grenfell, A. Kleczkowski, S. Ellner, B.M. Bolker, Measles as a case study in nonlinear forecasting and chaos, Philos. Trans. Roy. Soc. Lond. A 348 (1994) 515–530.

[38] B. Finkenstädt, B. Grenfell, Time series modelling of childhood diseases: a dynamical systems approach, J. Roy. Stat. Soc. C 49 (2000) 187–205.
[39] P. Rohani, D.J.D. Earn, B.T. Grenfell, The impact of immunisation on pertussis transmission in England and Wales, Lancet 355 (2000) 285–286.
[40] A. Sumi, N. Ohtomo, Y. Tanaka, A. Koyama, K. Satio, Comprehensive spectral analysis of time series data of recurrent epidemics, Jpn. J. Appl. Phys. 36 (1997) 1303–1318.
[41] W.P. London, J.A. Yorke, Recurrent outbreaks of measles, chickenpox and mumps. I. Seasonal variation in contact rates, Am. J. Epidemiol. 98 (1973) 453–468.
[42] S. Ellner, P. Turchin, Chaos in a noisy world: new methods and evidence from time series analysis, Am. Nat. 145 (1995) 343–375.
[43] M.J. Keeling, B.T. Grenfell, Stochastic dynamics and a power law for measles variability, Philos. Trans. Roy. Soc. Lond. B 354 (1999) 768–776.
[44] J.R. Gog, I. Oprea, M.R.E. Proctor, A.M. Rucklidge, Destabilization by noise of transverse perturbations to heteroclinic cycles: a simple model and an example from dynamo theory, Proc. Roy. Soc. Lond. A 455 (1999) 4205–4222.
[45] H.W. Hethcote, An age-structured model for pertussis transmission, Math. Biosci. 145 (1997) 89–136.
[46] B.T. Grenfell, Chance and chaos in measles dynamics, J. Roy. Stat. Soc. B 54 (1992) 383–398.
[47] H.B. Wilson, D.A. Rand, Detecting chaos in a noisy time-series, Proc. Roy. Soc. Lond. B 253 (1993) 239–244.